Neuron, Volume *100*

Supplemental Information

Subtype Diversification and Synaptic Specificity of Stem Cell-Derived Spinal Interneurons

Phuong T. Hoang, Joshua I. Chalif, Jay B. Bikoff, Thomas M. Jessell, George Z. Mentis, and Hynek Wichterle

SUPPLEMENTARY FIGURES

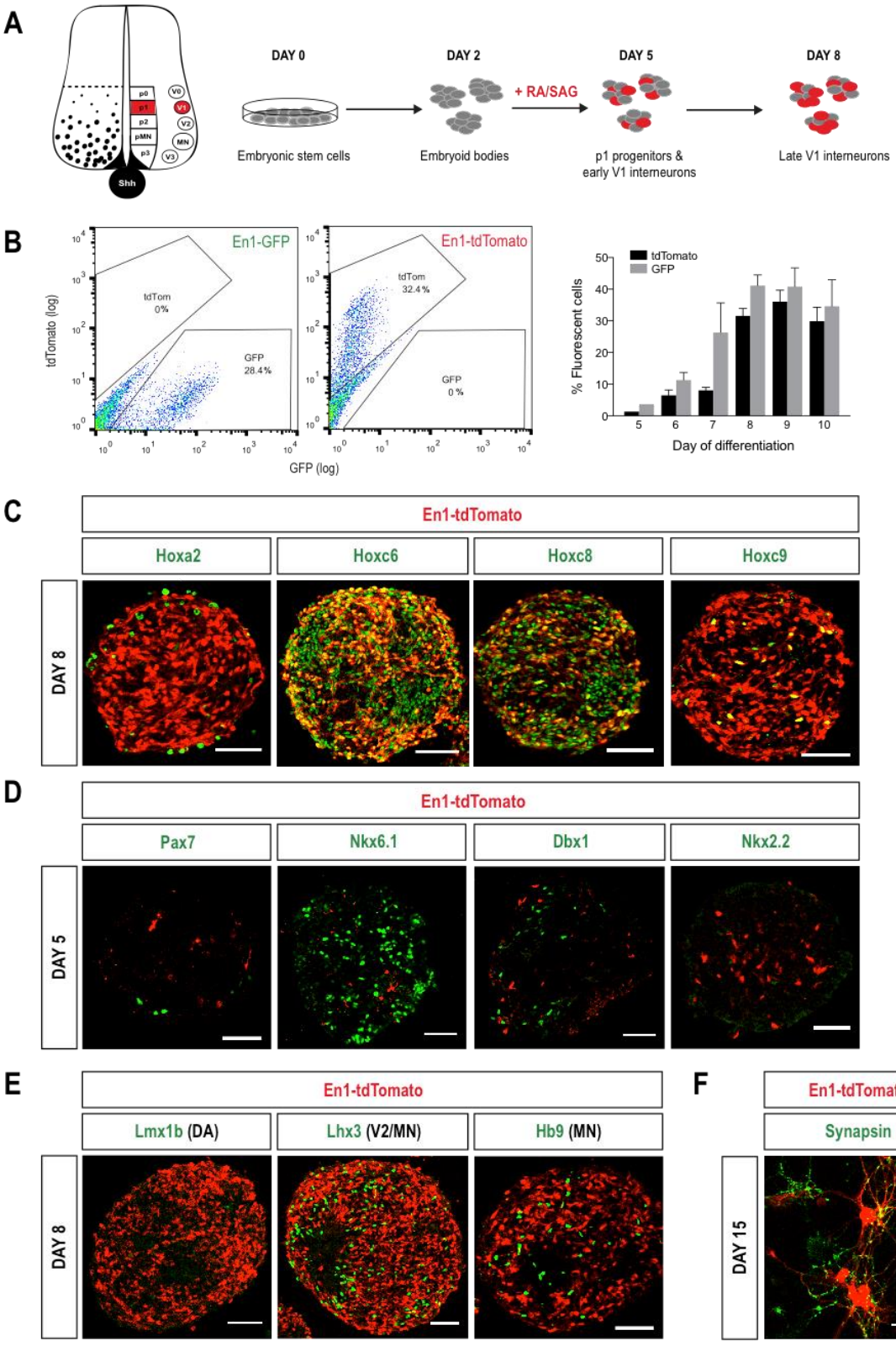

Figure S1. Differentiation of spinal V1 INs from mouse stem cells, Related to Figure 1.
(A) Strategy for differentiating ESCs to V1 INs using 1 μM retinoic acid (RA) for neuralization and posteriorization and 5 nM smoothened agonist (SAG) for ventralization of neural progenitors in embryoid bodies (EB). **(B)** Flow cytometry with quantification of *En1*-lineage cells from dissociated En1-GFP (left) or En1-tdTomato (right) on days 5-10 of differentiation (n=3; mean ± SEM). **(C)** Differentiation of ESCs using RA and low concentration of SAG (5 nM) results in cells with cervical and brachial spinal *Hox* expression profile. Scale bars, 50 μm. **(D)** Referring to Fig1D, day 5 EBs have low expression of non-p1 progenitor domain genes (*Pax7, Nkx6.1, Dbx1, and Nkx2.2*). Scale bars, 50 μM. **(E)** EBs do not express Lmx1b, a marker of *En1*-derived midbrain dopaminergic neurons; the V2 IN/MN marker Lhx3; or the MN marker Hb9. Scale bars, 50 μM. **(F)** *En1*-lineage neurons also express synaptic proteins such as Synapsin on culture day 15. Scale bar, 20 μM.

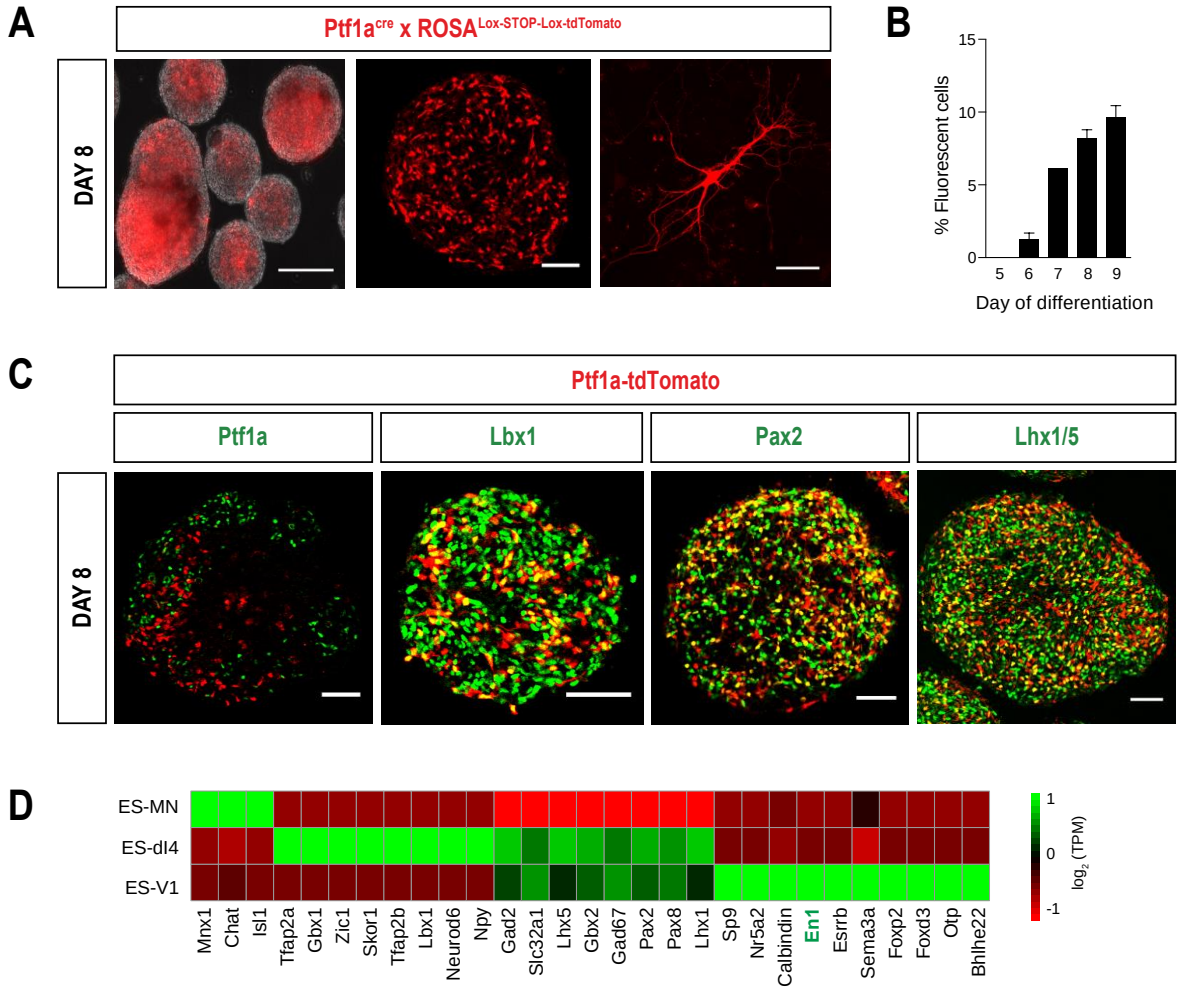

Figure S2. Directed differentiation of Ptf1a-derived dI4 interneurons, Related to Figure 2. **(A)** ESC lines were derived from *Ptf1a::cre* mice crossed to *ROSA-lsl-tdTomato* (Ptf1a-tdTomato). Treatment of day 2 EBs with 1 µM RA alone yields ~10% Ptf1a-tdTomato cells. Shown are day 8 EBs in suspension with live reporter expression (left); fixed, with endogenous reporter expression (middle); dissociated and cultured, with endogenous reporter expression. Scale bars, 50 µm. **(B)** Quantification of fluorescent cells from dissociated Ptf1a-tdTomato EBs over days 5-9 of differentiation (mean ± SEM). **(C)** ESC differentiation using RA leads to the induction of markers of postmitotic dI4 INs *in vivo* by day 8. Scale bars, 50 µm. **(D)** RNA-seq gene expression profiling of FACS-purified ESC-derived MNs (day 6), dI4 INs (day 8), and V1 INs (day 8) reveals cell type-specific expression of selected enriched genes for each cell type.

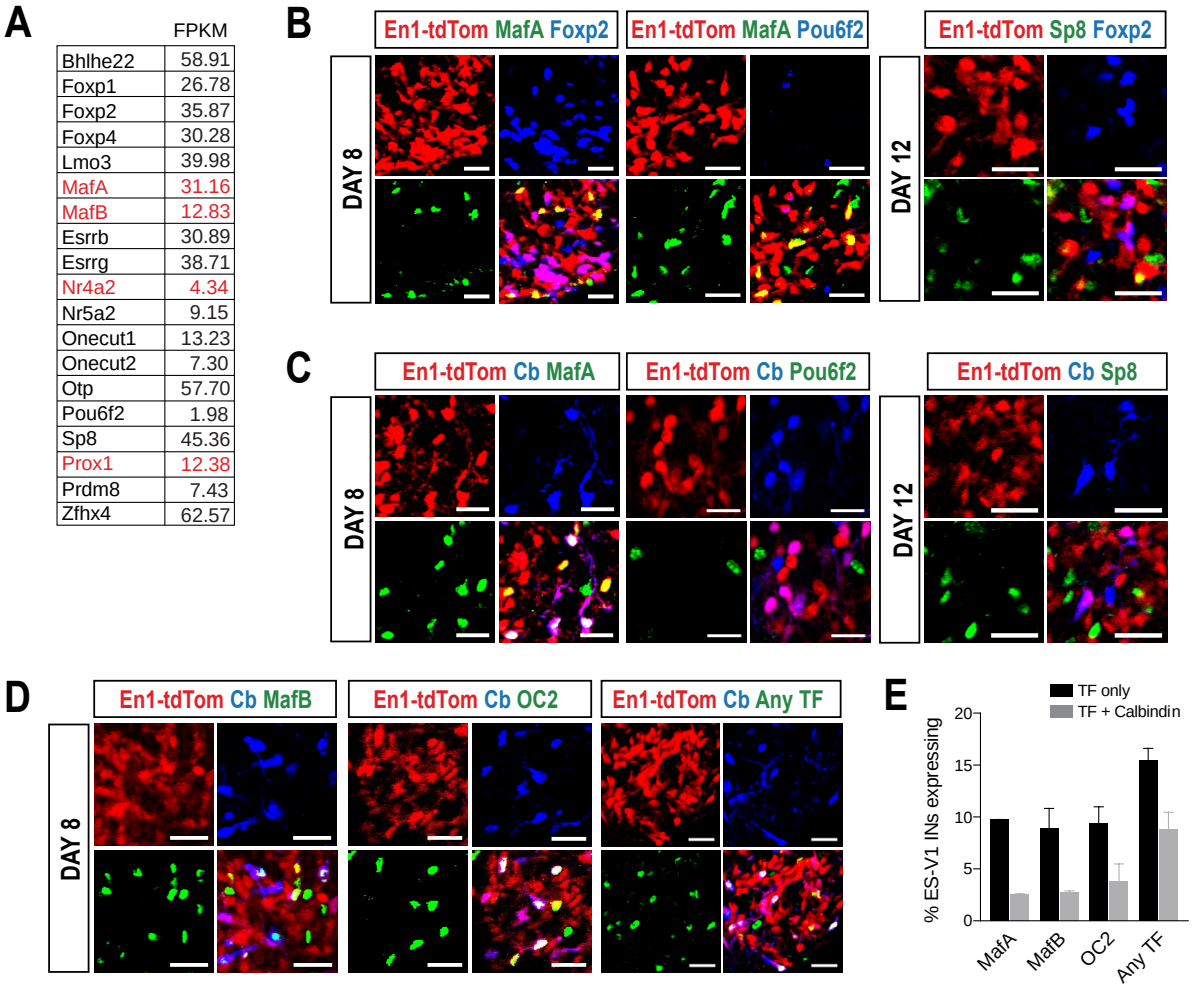

Figure S3. Molecular characterization of *in vitro* V1 interneuron clades, including MafA-related Renshaw cells, Related to Figure 3.

(A) RNA-seq FPKM values of TFs expressed in day 8 ES-V1 INs. All 19 TFs, including MafA, MafB and Prox1, are abundantly expressed in ES-V1 INs. **(B)** V1 IN clade-specific TFs (MafA, Foxp2, Pou6f2, and Sp8) have non-overlapping expression in En1-tdTomato cells. Scale bars, 20 µm. **(C, D)** Referring to Fig3E, subsets of Cb+ ES-V1 INs co-express MafA, MafB, and OC2, but not Pou6f2 or Sp8. **(E)** Quantification of ES-V1 INs expressing MafA, MafB, OC2 TFs only or TFs with Calbindin (mean ± SEM) (left). Quadruple immunostaining of MafA, MafB and OC2 with or without Calbindin ("Any TF") (right).

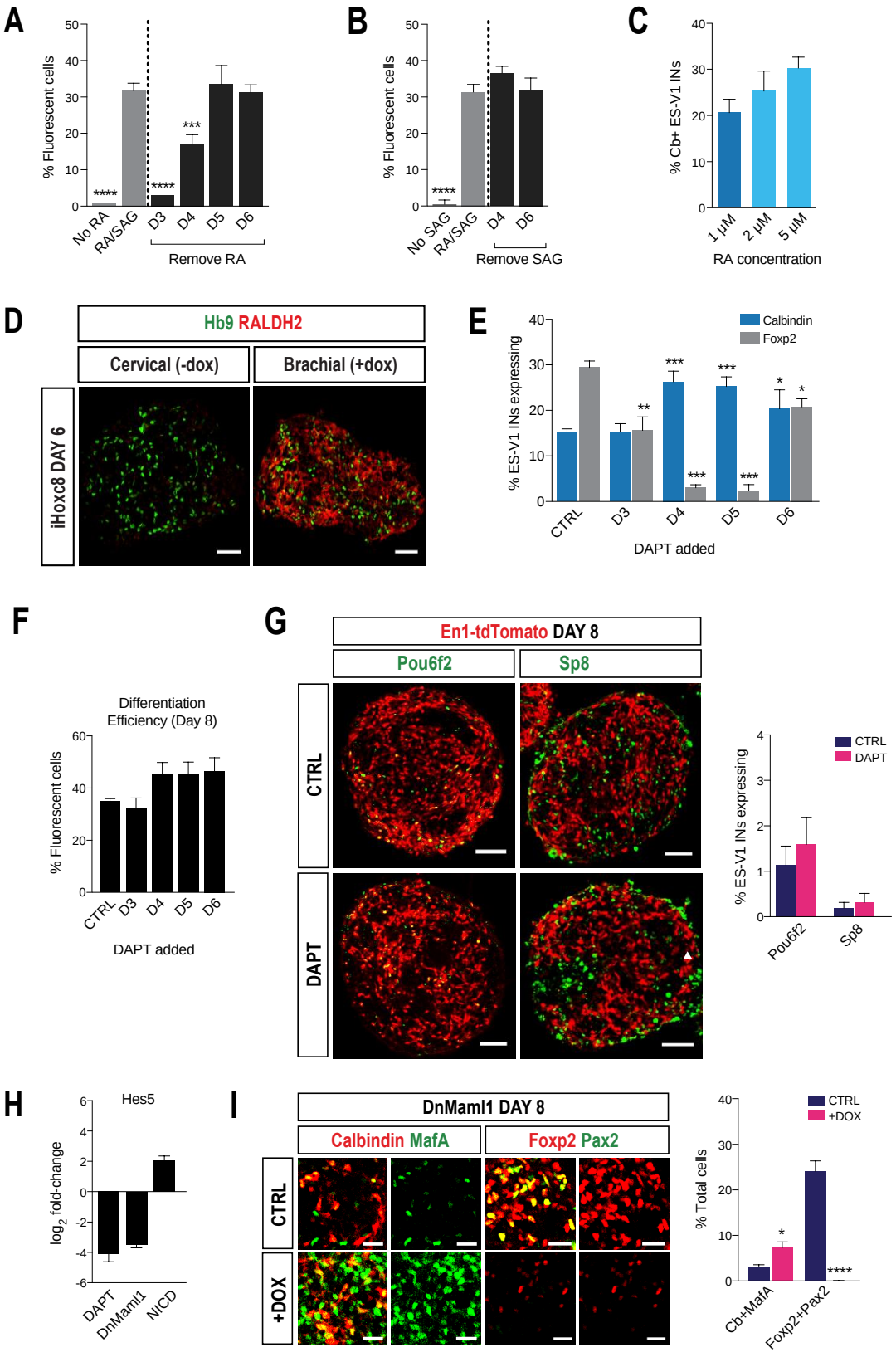
A
% Fluorescent cells
No RA
RA/SAG
D3
D4
D5
D6
Remove RA
B
% Fluorescent cells
No SAG
RA/SAG
D4
D6
Remove SAG
C
% Cb+ ES-V1 INs
1 µM
2 µM
5 µM
RA concentration
D
Hb9 RALDH2
Cervical (-dox)
Brachial (+dox)
iHoxc8 DAY 6
E
Calbindin
Foxp2
% ES-V1 INs expressing
CTRL
D3
D4
D5
D6
DAPT added
F
Differentiation Efficiency (Day 8)
% Fluorescent cells
CTRL
D3
D4
D5
D6
DAPT added
G
En1-tdTomato DAY 8
Pou6f2
Sp8
CTRL
DAPT
CTRL
DAPT
% ES-V1 INs expressing
Pou6f2
Sp8
H
Hes5
log2 fold-change
DAPT
DnMaml1
NICD
I
DnMaml1 DAY 8
Calbindin MafA
Foxp2 Pax2
CTRL
+DOX
CTRL
+DOX
% Total cells
Cb+MafA
Foxp2+Pax2

Figure S4. Molecular signals controlling V1 IN subtype identity, Related to Figure 4.
(A) Temporal requirement of retinoic acid (RA) signaling in V1 neurogenesis. Removal of RA on days 3 and 4 leads to diminished generation of En1-tdTomato cells. Removal of RA on days 5 and 6 produces similar numbers of En1-tdTomato cells as when RA is maintained throughout differentiation (mean ± SEM; ANOVA, ***p<0.01, ****p<0.0001). **(B)** Removal of SAG on day 4 or 6 does not affect ES-V1 IN differentiation. (ANOVA, ****p<0.0001). **(C)** Increased RA (2 μM or 5 μM) compared to control (1 μM) promotes the generation of Cb-expressing cells in a dose-dependent manner. **(D)** Referring to Fig4C, addition of doxycycline on late day 3 of ES-MN differentiation results in robust induction of the Hox gene *Hoxc8*, producing a homogenous population of brachial MNs highly enriched in the RA-synthesizing enzyme Raldh2. Scale bars, 50 μM. **(E)** Quantification of DAPT effect on generation of Cb-expressing versus Foxp2-expressing V1 INs in day 8 EBs (mean ± SEM; ANOVA, *p<0.05, **p<0.01, **p<0.001). **(F)** Notch inhibition with DAPT on days 4-6 does not significantly change generation of ES-V1 INs on day 8 (mean ± SEM). **(G)** Expression of Pou6f2 and Sp8 TFs in day 8 EBs in control versus DAPT treated (day 4) conditions. Scale bars, 50 μm. Mean ± SEM**. (H)** qPCR results showing that downregulation of Notch signaling using pharmacological DAPT treatment or inducible DnMaml1 in differentiating ES-V1 INs results in decreased relative expression of *Hes5*, a downstream target of Notch signaling, while activation of Notch using inducible NICD causes upregulation of *Hes5* (mean ± SEM). **(I)** Addition of dox on late day 3 to induce DnMaml1 expression in differentiating ES-V1 INs results in a significant increase in Cb/MafA-expressing cells (% total cells), with loss of Foxp2/Pax2-expressing cells (% total cells) in day 8 EBs (mean ± SEM; *Student's t-test,* *p<0.05, ****p<0.0001). Scale bars, 20 μM.

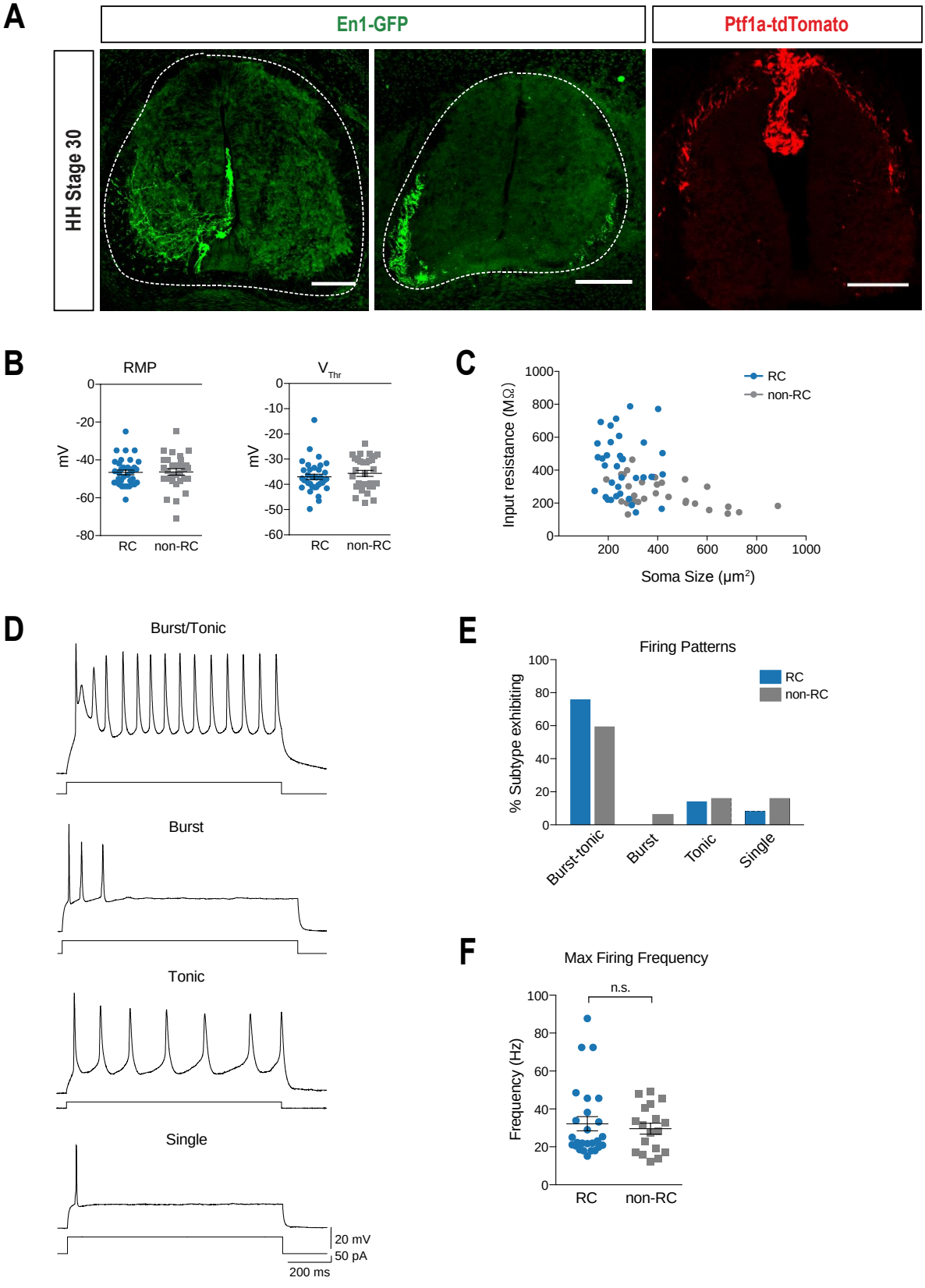
A
En1-GFP
Ptf1a-tdTomato
HH Stage 30
B
RMP
mV
0
-20
-40
-60
-80
RC
non-RC
V_Thr
mV
0
-10
-20
-30
-40
-50
-60
RC
non-RC
C
Input resistance (MΩ)
1000
800
600
400
200
0
200
400
600
800
1000
Soma Size (μm²)
RC
non-RC
D
Burst/Tonic
Burst
Tonic
Single
20 mV
50 pA
200 ms
E
Firing Patterns
% Subtype exhibiting
100
80
60
40
20
0
RC
non-RC
Burst-tonic
Burst
Tonic
Single
F
Max Firing Frequency
n.s.
Frequency (Hz)
100
80
60
40
20
0
RC
non-RC

Figure S5. ESC-derived Renshaw cells acquire distinct functional characteristics, including axon targeting and electrophysiological firing properties, Related to Figure 5.
(A) Axon trajectories of transplanted ES-V1 INs (left, middle) compared to ES-dI4 INs (right). Scale bars, 100 µm. **(B)** Referring to Fig5H, RCs (blue dots) and non-RC V1 INs (grey squares) have similar resting membrane and threshold potentials (mean ± SEM; *Student's t-test*, *$p<0.05$, ***$p<0.001$). **(C)** Scatterplot depicting relationship between soma size and input resistance for RC versus non-RC V1 INs. **(D)** Examples of burst/tonic ("repetitive"), burst, tonic and single action potential firing elicited in ES-RCs cultured for 2 weeks on astrocyte monolayer. **(E)** Total numbers of RCs that fired in burst/tonic, burst, tonic, and single action potential patterns compared to non-RC V1 INs. **(F)** There is no significant difference in maximum firing frequency between RCs and non-RCs (mean ± SEM).

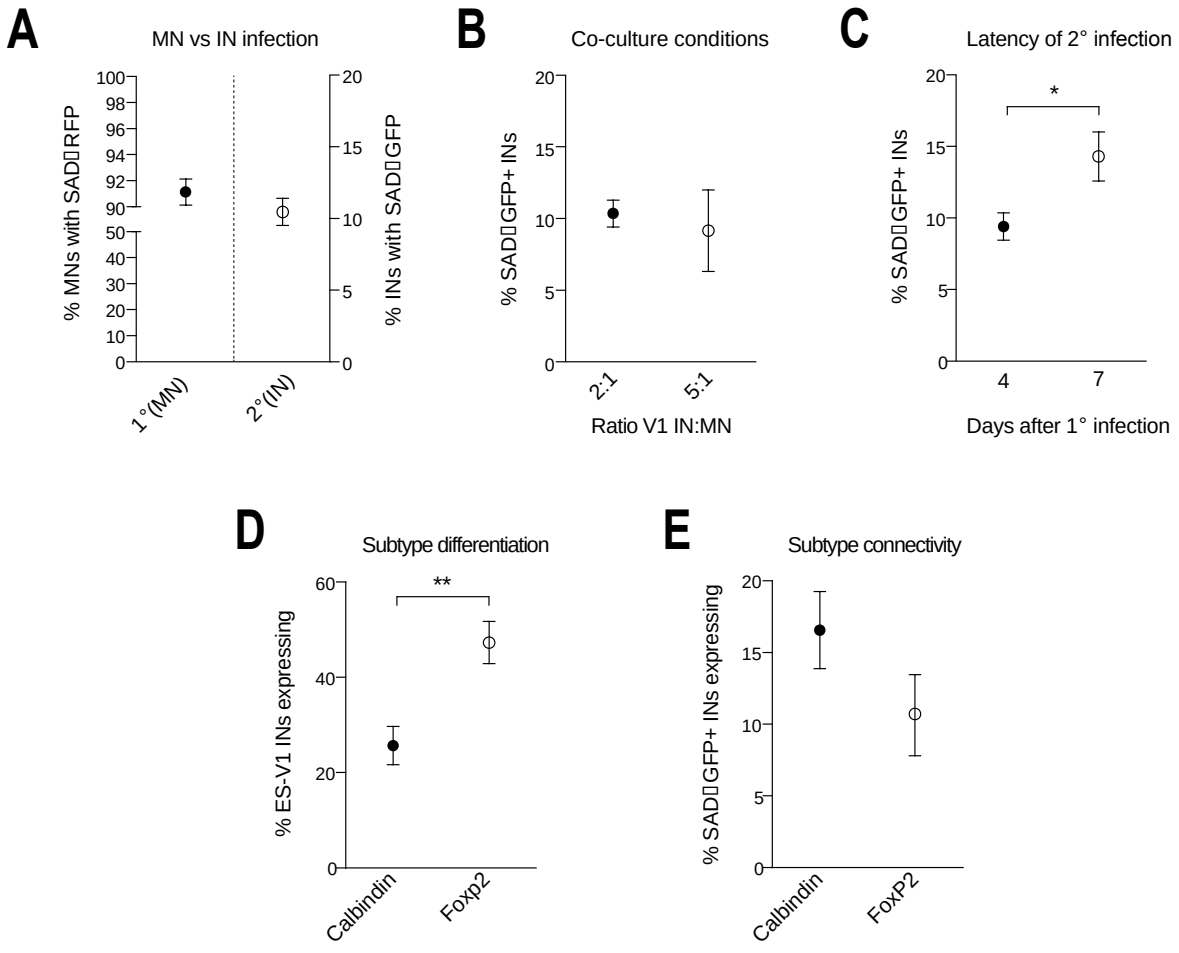

Figure S6. *In vitro* rabies virus labeling of monosynaptic connections between motor neurons and different V1 interneuron subtypes, Related to Figure 6.
(A) Efficiency of initial RABV infection in MNs compared to secondary infection in ES-V1 INs. Note the different y-axes. Mean ± SEM. **(B)** Efficiency of secondary infection of ES-V1 INs based on ratio of INs to MNs (see Supplementary Methods for further details). Mean ± SEM. **(C)** Longer duration of culture results in significantly higher % of ES-V1 INs forming monosynaptic connections with MNs (mean ± SEM; *Student's t-test*, *$p<0.05$). **(D)** Referring to Fig6D, under non-DAPT conditions, there are ~2X as many Foxp2-expressing ES-V1 INs generated as Cb-expressing ES-V1 INs (mean ± SEM; *Student's t-test*, **$p<0.01$). **(E)** There is a slight increase in Cb-expressing premotor ES-V1 INs compared to Foxp2-expressing ES-V1 INs. This data is combined with the differentiation efficiency in Figure S6D to calculate the connectivity index. Mean ± SEM.

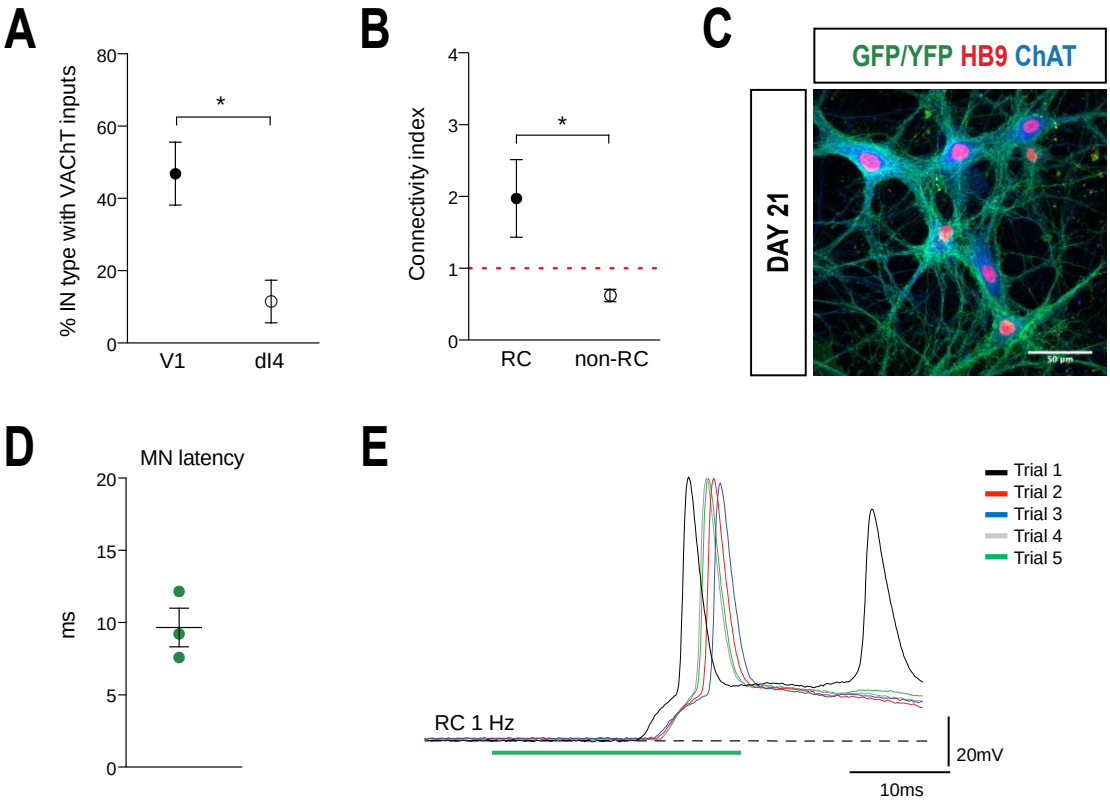

Figure S7. Analysis of synaptic connectivity in co-cultures of ESC-derived V1 interneurons and motor neurons, Related to Figure 7.
(A) Quantification of VAChT-immunoreactive inputs on ES-V1 versus dI4 INs (mean ± SEM; *Student's t-test*, *p<0.05). **(B)** Connectivity index for VAChT inputs on RCs versus non-RCs (mean ± SEM; *Student's t-test*, *p<0.05). **(C)** ESC line expressing *Hb9::CD14-IRES-GFP* for MN identification, and *CAG::ChR2-YFP* for optogenetic stimulation (Bryson et al., 2014). Dissociated MNs are immunostained for MN-specific markers choline acetyltransferase (ChAT) and Hb9. **(D)** Referring to Fig7G, MN latency to fire an action potential following photostimulation at 0.1 Hz frequency (measured from light onset to peak of the action potential). **(E)** Referring to Fig7I, response onset variability, or jitter, of the ES-RC response over multiple trials at 1 Hz (*Student's t-test*, *p<0.05).